

A comparison study of pathological features and drug efficacy between *Drosophila* models of C9orf72 ALS/FTD

Davin Lee^{1,†}, Hae Chan Jeong^{1,†}, Seung Yeol Kim², Jin Yong Chung², Seok Hwan Cho², Kyoung Ah Kim¹, Jae Ho Cho¹, Byung Su Ko¹, In Jun Cha³, Chang Geon Chung⁴, Eun Seon Kim^{1,*}, and Sung Bae Lee^{1,*}

¹Department of Brain Sciences, Daegu Gyeongbuk Institute of Science and Technology (DGIST), Daegu 42988, Republic of Korea, ²SK Biopharmaceuticals Co., Ltd., Seongnam 13494, Republic of Korea, ³Brain Research Policy Center, Korea Brain Research Institute, Daegu 41068, Republic of Korea, ⁴Department of Neurology, Johns Hopkins University School of Medicine, Baltimore, MD 21205, USA

*Correspondence: eunseon_k@dgist.ac.kr (ESK); sblee@dgist.ac.kr (SBL)

<https://doi.org/10.1016/j.mocell.2023.12.003>

ABSTRACT

Amyotrophic lateral sclerosis is a devastating neurodegenerative disease with a complex genetic basis, presenting both in familial and sporadic forms. The hexanucleotide (G₄C₂) repeat expansion in the *C9orf72* gene, which triggers distinct pathogenic mechanisms, has been identified as a major contributor to familial and sporadic Amyotrophic lateral sclerosis cases. Animal models have proven pivotal in understanding these mechanisms; however, discrepancies between models due to variable transgene sequence, expression levels, and toxicity profiles complicate the translation of findings. Herein, we provide a systematic comparison of 7 publicly available *Drosophila* transgenes modeling the G₄C₂ expansion under uniform conditions, evaluating variations in their toxicity profiles. Further, we tested 3 previously characterized disease-modifying drugs in selected lines to uncover discrepancies among the tested strains. Our study not only deepens our understanding of the *C9orf72* G₄C₂ mutations but also presents a framework for comparing constructs with minute structural differences. This work may be used to inform experimental designs to better model disease mechanisms and help guide the development of targeted interventions for neurodegenerative diseases, thus bridging the gap between model-based research and therapeutic application.

© 2023 The Authors. Published by Elsevier Inc. on behalf of Korean Society for Molecular and Cellular Biology. This is an open access article under the CC BY-NC-ND license (<http://creativecommons.org/licenses/by-nc-nd/4.0/>).

Keywords: Amyotrophic lateral sclerosis, *C9orf72*, Comparison study, Drug screening, G₄C₂ repeat expansion models

INTRODUCTION

Amyotrophic lateral sclerosis (ALS) is a progressive neurodegenerative disorder that primarily affects motor neurons in the brain and spinal cord, resulting in muscle weakness, paralysis, and eventual death (DeJesus-Hernandez et al., 2011). Central to ongoing research efforts is the determination to better comprehend the genetic contributors of ALS (Byrne et al., 2013; Kwiatkowski et al., 2009; Rosen et al., 1993; Shatunov et al., 2010). Although only 5% to 10% of ALS cases are familial (Majounie et al., 2012), a significant percentage of sporadic cases also present genetic cause (Van Daele et al., 2023), prompting extensive inquiries into unraveling the genetic underpinnings and complex pathogenesis of ALS.

One of the major breakthroughs in ALS research is the identification of the hexanucleotide (G₄C₂) repeat expansion in the *C9orf72* gene, which accounts for the largest proportion

of familial ALS cases (DeJesus-Hernandez et al., 2011). The expansion results in reduced expression of the *C9orf72* gene (Shi et al., 2018) as well as the formation of RNA foci, which are accumulations of transcribed repeat RNA (Zu et al., 2013). These RNA foci are found to sequester RNA-binding proteins and disrupt RNA processing and splicing (Lee et al., 2013). Furthermore, the transcribed RNA from the G₄C₂ expansion forms stable G-quadruplex structures. Interestingly, the repeat expansion triggers an unusual repeat-associated non-AUG (RAN) translation, producing dipeptide repeat (DPR) proteins that are prone to aggregation and toxic to various cellular components (Ash et al., 2013). Notably, this same mutation is also observed in frontotemporal dementia (FTD) (Ash et al., 2013; Devenney et al., 2014), suggesting that advancements made in G₄C₂ pathogenesis could have broader implications for understanding and treating both ALS and FTD.

Given the complex characteristics of the G₄C₂ repeat expansion in the *C9orf72* gene, numerous animal models have

[†] These authors contributed equally to this work.

been generated to accurately represent the disease (Batra and Lee, 2017). In fact, animal models expressing disease-associated transgenes have been instrumental in elucidating the complexities of G_4C_2 -mediated disease pathogenesis. These models enabled us to study how ALS or other G_4C_2 -associated neurodegenerative diseases progress *in vivo* and discover potential therapeutic interventions. However, these transgenic animal models are not without limitations.

In many animal models, transgenes are usually overexpressed to a nonphysiological level due to the usage of strong promoters and the absence of regulatory sequences that are normally present in the untranslated regions. This can lead to exaggerated phenotypic results, creating disparities between animal models and human disease. Importantly, minute differences in the transgene configuration can have consequential effects on the observed disease phenotype. For example, while most G_4C_2 transgene constructs use uninterrupted pure G_4C_2 repeats, the $(G_4C_2)_{44}$ construct includes an intronic 5' leader sequence (LDS), an attempt to more closely mimic the genetic configuration observed in ALS patients, leading to notable differences in DPR expression and toxicity (Goodman et al., 2019b; Kearsse et al., 2016). This diversity, while valuable for studying specific aspects of the disease, complicates the comparison and interpretation of results across studies. Further confounding the issue is the variability in toxic profiles, such as the expression of DPR(s), across models, which makes it difficult to delineate the relative contributions of each pathogenic mechanism and identify potential therapeutic targets.

Therefore, it is imperative to undertake an unbiased and systematic comparison of available transgenes of G_4C_2 , assessing the toxic profiles and variations in transgene constructs. This endeavor not only enhances our understanding of C9orf72- G_4C_2 mutations but also establishes a framework for assessing constructs with minute structural differences that can have significant consequences. Such a framework is essential for informing experimental designs that accurately model disease mechanisms and guiding the development of targeted therapeutic interventions. In this article, we contribute to this vital area by providing a comparative analysis of 7 publicly available *Drosophila* transgenes that model the G_4C_2 expansion. We also established a framework wherein we conducted phenotype testing under uniform conditions, ensuring that the transgenes were subjected to comparable environments, thereby enabling a more precise and controlled analysis of their toxicity profiles. Through our analysis, we aim to offer insights into the molecular consequences of variations in transgene constructs and underscore the nuances that should be considered in future studies involving G_4C_2 expansion modeling. Ultimately, these comparative analyses and the framework developed may help underpin a more comprehensive understanding of the molecular mechanisms at play, which is fundamental for the advancement of targeted strategies in the management and treatment of neurodegenerative diseases.

MATERIALS AND METHODS

Drosophila Stocks

Flies were maintained at 27°C. The following lines were obtained from Bloomington *Drosophila* Stock Center: *Elav-Gal4*

(8765), *GMR-Gal4* (1104), *UAS-luciferase* (35788), *UAS-(G₄C₂)₃₆* (58688), *UAS-LDS-(G₄C₂)₄₄.GR-GFP/TM3* (84723), *UAS-(G₄C₂)₄₉/TM6C* (84726), *UAS-(G₄C₂)₄₉* (84727). Using a transposon-based approach, the *GMR-Gal4* (III) was generated by relocating transgene from its original position on the second chromosome to the third chromosome. *UAS-(G₄C₂)₃₀/cyo* and *UAS-(G₄C₂)₃₀/Tm3* were provided by Peng Jin (Emory University). *UAS-(G₄C₂)₁₆₀* line was provided by Fen-Biao Gao (University of Massachusetts).

Molecular Cloning and Generation of Transgenic Flies

UAS-HA-Rhau was synthesized and subcloned into pACU2 vectors using *NOTI* and *XbaI*, and the HA epitope was added at the N-terminus. Transgenic flies were generated by BestGene, Inc. Nucleotide sequences are available upon request.

Immunohistochemistry for Fly Brain

As previously described by Cho et al. (2022), Park et al. (2020), and Ryu et al. (2022), adult flies were dissected in Schneider's insect medium (Cat No. S0146; Sigma) to obtain brain samples for immunohistochemical analysis. Brains were fixed with 3.7% formaldehyde for 20 minutes at room temperature (RT). After washing with PBST (0.3% Triton-X100 in phosphate-buffered saline), brains were incubated in a blocking buffer (5% Normal donkey serum in 0.3% PBST) for 1 hour at RT. Next, the brains were incubated in the primary antibody overnight at 4°C. The following primary antibodies were used in this study: α -glycine-proline (GP) rabbit (Proteintech, 24494-I-AP) at 1:200 concentration, α -ribosomal RNA (rRNA) (Y10b) mouse (NOVUS, NB100-662) at 1:200 concentration, α -dTDP-Gly rabbit (gift by James Shen at Taipei Medical University) at 1:200 concentration. Brains were then washed with PBST 3 times for 10 minutes each. Then, brains were further incubated in the secondary antibody for 2 hours at RT. The following secondary antibodies were used: α -rb alexa555 (Thermo Fisher Scientific, Z25305) at 1:200 concentration, α -rb alexa647 (Invitrogen, A21244) at 1:200 concentration, α -mouse alexa647 (Invitrogen, A21236) at 1:200 concentration, α -rb alexa488 (Abcam, A11034) at 1:200 concentration. Brains were washed 5 times with PBST, and Antifade Mounting Medium with 4',6-diamidino-2-phenylindole (DAPI, H-1200, VECTASHILD) was used.

RNA Extraction and Quantitative Real-time Polymerase Chain Reaction (qRT-PCR)

RNA extraction and complementary DNA (cDNA) synthesis of fly samples were performed as previously described (Chung et al., 2017; Lee et al., 2022, 2023). Total RNAs were extracted from adult fly heads using Easy-Blue system (iNtRON Biotechnology). cDNAs were synthesized from 3 μ g of total RNAs using GoScript Reverse Transcription (Promega, A2791) according to the manufacturer's standard protocol. Quantitative PCR experiments were performed using the synthesized cDNAs with QuantiSpeed SYBR Green kit (PhilKorea, QS105-10) and CFX96 Touch™ Real-Time PCR Detection System (Bio-Rad). Gene-specific primers were listed in Supplementary Figure S5a (Tran et al., 2015; Xu et al., 2013). *rp49* was used as a housekeeping gene to normalize the expression levels of target genes. mRNA fold change of each gene was calculated

using the comparative Ct method. Gene-specific primers were designed with Primer-BLAST (ncbi.nlm.nih.gov/tools/primer-blast) and *Drosophila* RNAi Screening Center FlyPrimerBank (flyrnai.org/flyprimerbank). Some primer sequences were obtained from published studies.

Conditions for Acquiring and Imaging Eye Phenotypes

7 days or 10 days after eclosion adult flies expressing G₄C₂ repeats under the control of *GMR-Gal4* at 27 °C were dissected to conduct their fly eyes and acquired with a Nikon Eclipse 90i. Adult flies expressing *Rhau* were grown at 25 °C and dissected 1 day after eclosion.

Negative Geotaxis Assay

Right after eclosion from the pupa, 15 flies of each genotype were collected and reared for, depending on the experiment, 3 days or 10 days at 27°C. After the assigned days, these flies were transferred to an acrylic cylinder closed at one end (3-cm diameter, 18-cm height) without CO₂ anesthesia, while the top of the cylinder was sealed with sponges to block escape. After 20 minutes of acclimation at RT, the flies were placed on the bottom of the cylinder by tapping the cylinder against a table, and climbing was recorded for 1 minute. Climbing ability was measured with a climbing index (proportion of 10 to 15 flies climbing > 10 cm from the bottom of the cylinder within 10 seconds) in each experimental group of flies.

Lifespan Assay

Lifespan assays were performed with guidance from a previous study (Pradhan et al., 2023). In each experiment, at least 100 male flies of each genotype were collected within 24 hours after pupal eclosion. Flies were maintained at low density (15 males per wide vial) at 27°C and transferred to new vials every 2 days. The number of dead flies was counted on a daily basis. Kaplan-Meier survival analysis was used. Statistical differences were assessed with the log-rank test.

Image Acquisition and Processing

All immunohistochemistry (IHC) samples were taken at 400× magnification, acquired by Zeiss LSM780 confocal microscopy (Zeiss). The posterior regions of mushroom body Kenyon cells in the fly brains were taken to examine the expression of DPRs. To quantify the signals of DPRs, the pixel intensities were measured by histogram analysis performed with Fiji.

Statistical Analyses

Statistical analysis was done using GraphPad Prism 7 (GraphPad Software). We applied Student's t-test, Log-rank (Mantel-Cox) test or 1-way Analysis of Variance (ANOVA) followed by Tukey's post-hoc analysis. *, **, ***, and **** represent **P* < 0.05, ***P* < 0.01, ****P* < 0.001, and *****P* < 0.0001. Ns is not significant. Error bars indicate standard error of the mean (SEM).

RESULTS

Comparative Analysis of the Neurotoxicity and Pathological Effects of Various G₄C₂ Constructs in *Drosophila* Models

To evaluate the respective toxicities and pathologies of publicly available G₄C₂ constructs (Table 1 and Supplementary Fig. S1a), we performed an in-depth comparative analysis in *Drosophila* using 2 different GAL4 drivers: *Elav-Gal4* and *GMR-Gal4*. Initially, we employed the *GMR-Gal4* driver to express the G₄C₂ constructs in the *Drosophila* eye, a well-established model for studying neurodegeneration. Using the degeneration severity criteria detailed in Supplementary Figure S1b, degeneration scores revealed that 2 lines had significantly higher scores compared to the other constructs (Fig. 1a and b). While most G₄C₂ constructs, apart from (G₄C₂)₁₆₀, generated significant degenerative eye phenotypes, flies expressing (G₄C₂)₃₀ (II) and (G₄C₂)₃₆ demonstrated the most pronounced degeneration. Note that 2 (G₄C₂)₄₉ lines were excluded from the experiment due to their lethality when expressed in neurons or the eye at 27°C, thereby precluding further analysis.

Subsequently, we examined the climbing ability of the flies expressing different G₄C₂ constructs neuronally with the *Elav-Gal4* driver on days 3 and 10 to assess the progression of motor behavior impairments over time. As a pan-neuronal expression of (G₄C₂)₃₀ transgenes using *Elav-Gal4* (I) caused developmental lethality (Xu et al., 2013), we used the *Elav-Gal4* (II) driver, a previously described non-lethal *Elav-Gal4* alternative (Wen et al., 2020), for our investigations. On day 3, both (G₄C₂)₃₀ lines demonstrated substantial toxicity, significantly impairing the climbing ability of the flies (Fig. 1c). By day 10, the *LDS*-(G₄C₂)₄₄ line was the most affected among the flies that survived until adulthood, showing the steepest decline in motor function over time among flies observed (Fig. 1d).

Finally, we assessed the lifespan of the flies expressing these constructs for a period of up to 30 days to measure the overall organismal health, complementing the relative short-term phenotypic effects observed in the eye and motor behavior assays. This revealed significant variations in the lifespan, with different constructs displaying differing levels of toxicity (Fig. 1e). Importantly, the *LDS*-(G₄C₂)₄₄ line was found to be the most toxic, evidenced by the shortest lifespan among all the constructs studied. Additionally, the (G₄C₂)₃₆ construct showed a moderate effect on lifespan when expressed in neurons using *Elav-Gal4*.

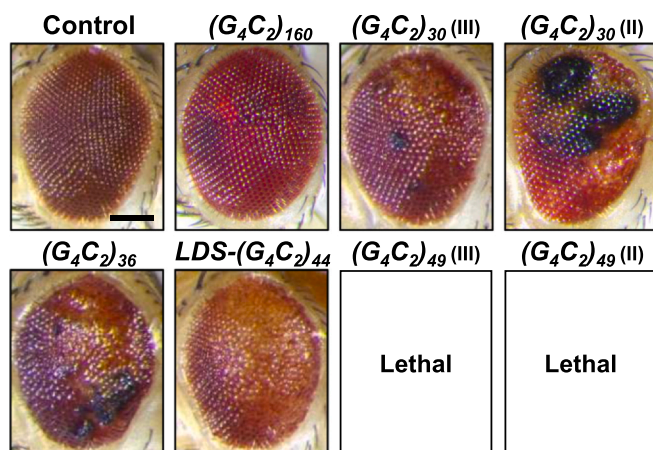
Our results illustrate that the expression of G₄C₂ repeat expansion constructs in *Drosophila* leads to notable neurotoxic effects, with varying levels of toxicity among different constructs. Particularly, the *LDS*-(G₄C₂)₄₄ line was highly toxic, exhibiting detrimental effects on both climbing and lifespan phenotypes while demonstrating a milder phenotype in eye degeneration. Moreover, the (G₄C₂)₃₀ (II) line was highly toxic in the climbing assay and eye degeneration, indicating impaired neuronal function, while the (G₄C₂)₃₆ showed consistent moderate toxicity in performed assays. These findings elucidate the neurotoxic impact of G₄C₂ repeat expansion constructs in *Drosophila*, highlighting the varying degrees of toxicity among different constructs.

Table 1. Characteristics of G₄C₂ constructs used in the study

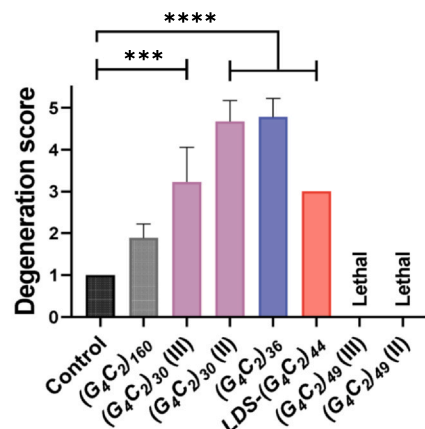
Identification		Transgene information			Reference-based toxicity			Reference (s)
BL number	Transgene	Repeats	Distinguishing features	AUG codon	Inserted chromosome	RNA foci	DPR	
NA	(G ₄ C ₂) ₁₆₀	160 Repeats	Intronic 160 G ₄ C ₂ repeat minigenes flanked by human intronic and exonic sequences	None	Chr 2.	Found (Tran et al., 2015)	Found GP (Tran et al., 2015)	Tran et al. (2015), Yuva-Aydemir et al. (2019)
NA	(G ₄ C ₂) ₃₀ (III)	30 Repeats	Uninterrupted pure repeats	None	Chr 3.	NA	NA	Xu et al. (2013), Dubey et al. (2022), Cunningham et al. (2020)
NA	(G ₄ C ₂) ₃₀ (II)	30 Repeats	Uninterrupted pure repeats	None	Chr 2.	NA	NA	
58688	(G ₄ C ₂) ₃₆	36 Repeats	Uninterrupted pure repeats	None	Chr 2, 25C6, 2-L:5108448.	Found (Mizielinska et al., 2014)	Found GR (Mizielinska et al., 2014)	Mizielinska et al. (2014)
84723	LDS-(G ₄ C ₂) ₄₄	44 Repeats	5' leader sequence (LDS) inserted immediately upstream of the G ₄ C ₂ repeats, 114 bp of sequence upstream of the repeat in intron 1 of C9orf72 in patients, and a 3' GFP tag in the GR reading frame.	None	Chr 3.	NA	GFP-tagged GR	Goodman et al. (2019b), Cunningham et al. (2020)
84726	(G ₄ C ₂) ₄₉ (III)	49 Repeats	Uninterrupted pure repeats	None	Chr 3.	Found (Kramer et al., 2016)	Found GP (Kramer et al., 2016)	Goodman et al. (2019a), Kramer et al. (2016)
84727	(G ₄ C ₂) ₄₉ (II)	49 Repeats	Uninterrupted pure repeats	None	Chr 2.	Found (Kramer et al., 2016)	Found GP (Kramer et al., 2016)	

BL, Bloomington Drosophila Stock Center; GR, Glycine-arginine; GP, Glycine-proline; DPR, dipeptide repeat; GFP, green fluorescent protein; NA, not applicable. For each line, the transgene information, distinguishing features, the presence of AUG codons, the chromosome in which the construct is inserted, the presence of RNA foci (literature-based), the presence of DPR proteins (literature-based), the observation of toxicity (literature-based), and relevant references are provided.

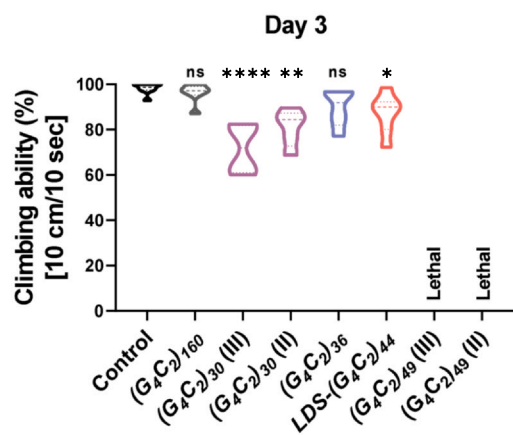
a



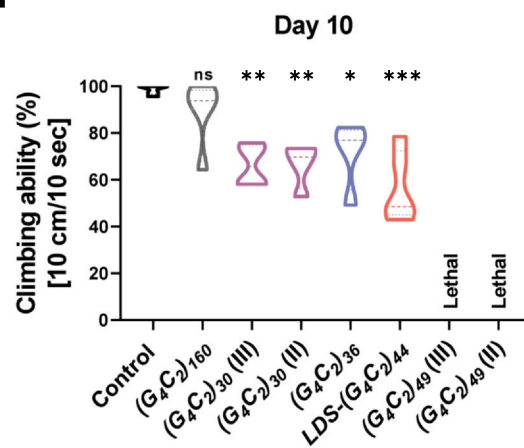
b



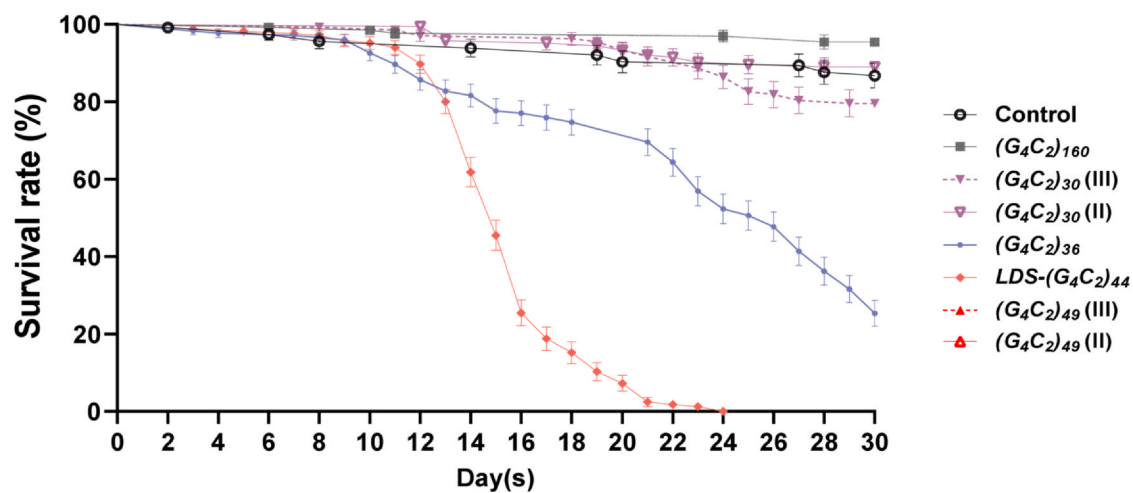
c



d



e



(caption on next page)

Fig. 1. Comparative analysis of the neurotoxicity and pathological effects of various G_4C_2 constructs in *Drosophila* models. (a) Representative images of eye phenotype in *Drosophila* models expressing denoted G_4C_2 transgenes at day 7 APE (Genotype: Control, *GMR-Gal4/+;UAS-luciferase/+* | (G_4C_2)₁₆₀, *GMR-Gal4/UAS-(G₄C₂)₁₆₀+/+* | (G_4C_2)₃₀ (III), *GMR-Gal4/+;UAS-(G₄C₂)₃₀/+* | ($G_4C_2)₃₀ (II), *GMR-Gal4/UAS-(G₄C₂)₃₀+/+* | ($G_4C_2)₃₆, *GMR-Gal4/UAS-(G₄C₂)₃₆+/+* | *LDS-(G₄C₂)₄₄*, *GMR-Gal4/+;UAS-LDS-(G₄C₂)₄₄-GR-GFP/+* | (G_4C_2)₄₉ (III), *GMR-Gal4/+;UAS-(G₄C₂)₄₉/+* | ($G_4C_2)₄₉ (II), *GMR-Gal4/UAS-(G₄C₂)₄₉+/+*) (black scale bar, 100 μ m). (b) Quantification of eye phenotype in *Drosophila* expressing denoted G_4C_2 transgenes described in (a). The degeneration score was assigned based on the criteria provided in [Supplementary Figure S1b](#). (c) Quantification of climbing ability in *Drosophila* expressing denoted G_4C_2 transgenes at day 3 APE (Genotype: Control, *Elav-Gal4/+;UAS-luciferase/+* | (G_4C_2)₁₆₀, *Elav-Gal4/UAS-(G₄C₂)₁₆₀+/+* | (G_4C_2)₃₀ (III), *Elav-Gal4/+;UAS-(G₄C₂)₃₀/+* | ($G_4C_2)₃₀ (II), *Elav-Gal4/UAS-(G₄C₂)₃₀+/+* | ($G_4C_2)₃₆, *Elav-Gal4/UAS-(G₄C₂)₃₆+/+* | *LDS-(G₄C₂)₄₄*, *Elav-Gal4/+;UAS-LDS-(G₄C₂)₄₄-GR-GFP/+* | ($G_4C_2)₄₉ (III), *Elav-Gal4/+;UAS-(G₄C₂)₄₉/+* | ($G_4C_2)₄₉ (II), *Elav-Gal4/UAS-(G₄C₂)₄₉+/+*). (d) Quantification of climbing ability in *Drosophila* expressing denoted G_4C_2 transgenes described in (c) at day 10 APE. (e) Lifespan analysis of *Drosophila* expressing denoted G_4C_2 transgenes described in (c). Survival data were plotted using the Kaplan-Meier method. Both (G_4C_2)₄₉ lines were excluded from lifespan analysis due to lethality in our experimental conditions.$$$$$$$

Detection of GP DPRs and TAR DNA-binding protein-43 homolog (TBP) in the Brains of G_4C_2 -Expressing *Drosophila*

We found that the expression of 7 publicly available G_4C_2 repeat transgenes resulted in differing degrees of toxicity. Existing literature indicates a strong correlation between DPRs and neuronal toxicity (Lee et al., 2016; Mizielinska et al., 2014), which led us to hypothesize that elevated concentrations of DPR proteins could be observed in flies exhibiting the highest behavioral or cellular degeneration.

To test this hypothesis, we utilized a well-established DPR antibody specific to poly-GP repeats (Dafinca et al., 2016) as a representative DPR marker and observed its expression in the *Drosophila* central nervous system. In line with our hypothesis, we observed considerable GP DPRs in both (G_4C_2)₃₀ (II) and *LDS-(G₄C₂)₄₄* expressing fly lines, whereas other lines

exhibited relatively low GP DPR expression levels (Fig. 2a and b). Surprisingly, despite showing moderate phenotypic toxicity, the fly brains expressing (G_4C_2)₃₆ showed little to no evidence of GP DPR expression, possibly suggesting the involvement of other toxic DPRs, such as GR DPR (Mizielinska et al., 2014). Interestingly, the GP DPRs largely lacked the colocalization with DAPI staining, suggesting that GP DPRs, similar to previous findings (Goodman et al., 2019b), were expressed in the cytoplasm of Kenyon cells. In addition, to validate that signals from GP staining can be used as a representative marker for DPRs, we utilized the *LDS-(G₄C₂)₄₄* transgene and tracked the localization of GR DPR by detecting green fluorescent protein (GFP) signals in the brain. While significant GR expression was, as expected, observed, the GFP signals were predominantly in the Kenyon cell nucleus, contrary to the GP DPRs (Supplementary Fig. S2a). This suggests that DPR proteins predominantly

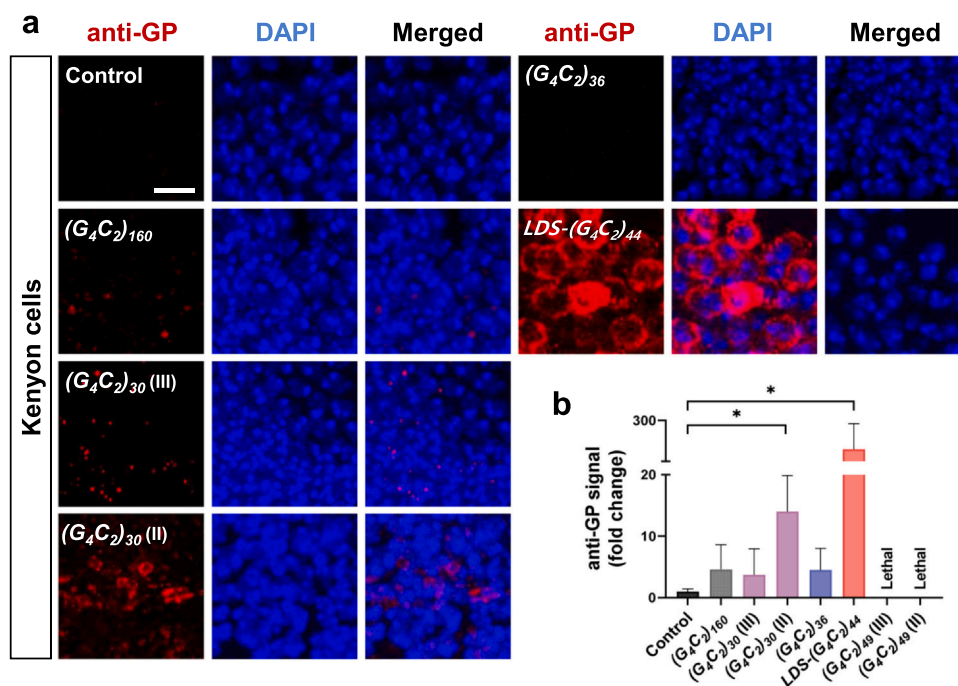
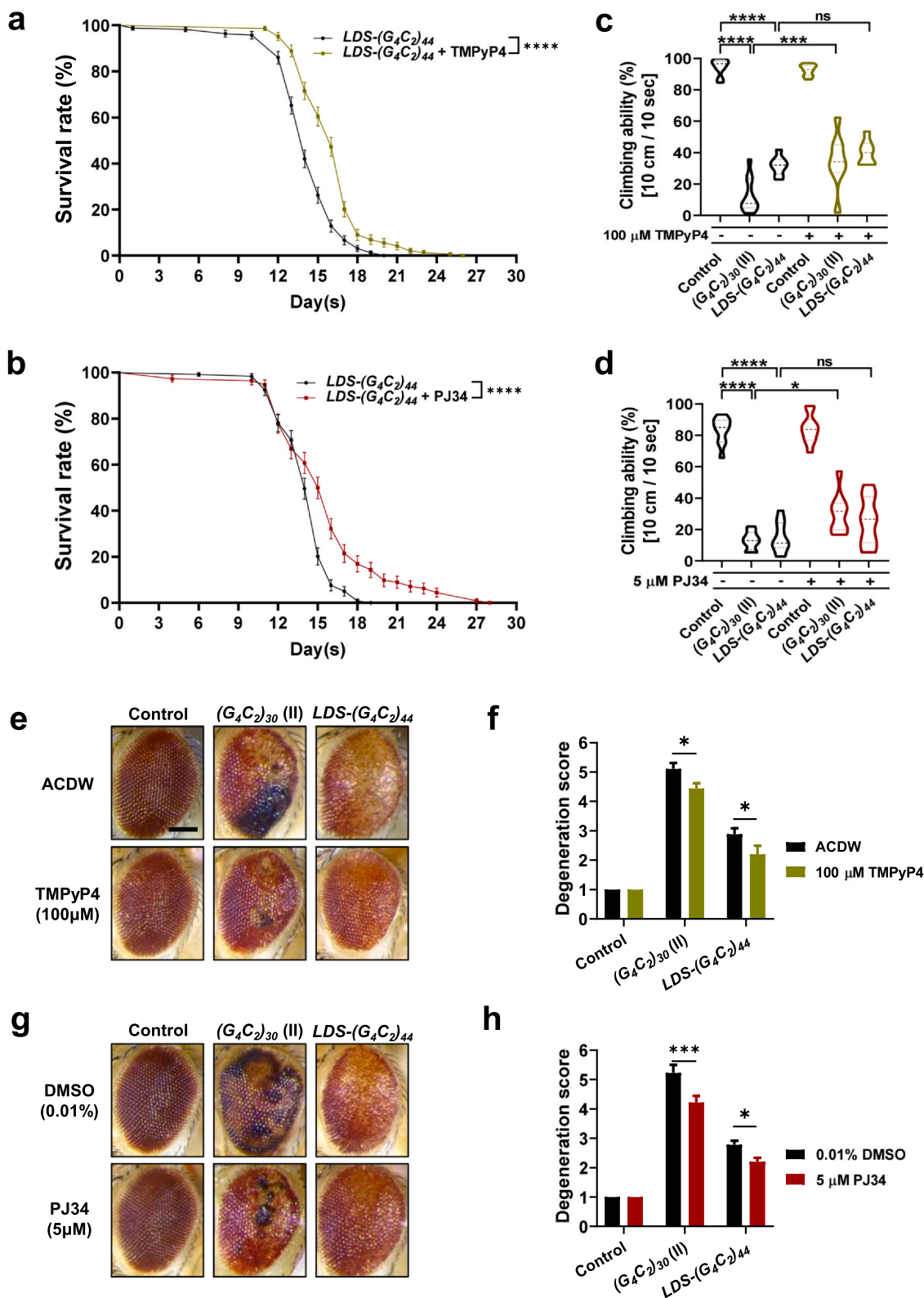


Fig. 2. Detection of GP DPRs in the brains of G_4C_2 -expressing *Drosophila*. (a) Representative images of GP staining in the Kenyon cells of *Drosophila* brains expressing G_4C_2 transgenes at day 10 APE. (Genotype: Control, *Elav-Gal4/+;UAS-luciferase/+* | (G_4C_2)₁₆₀, *Elav-Gal4/UAS-(G₄C₂)₁₆₀+/+* | ($G_4C_2)₃₀ (III), *Elav-Gal4/+;UAS-(G₄C₂)₃₀/+* | ($G_4C_2)₃₀ (II), *Elav-Gal4/UAS-(G₄C₂)₃₀+/+* | ($G_4C_2)₃₆, *Elav-Gal4/UAS-(G₄C₂)₃₆+/+* | *LDS-(G₄C₂)₄₄*, *Elav-Gal4/+;UAS-LDS-(G₄C₂)₄₄-GR-GFP/+*) (white scale bar, 5 μ m). (b) Quantification of GP DPR staining in *Drosophila* expressing denoted G_4C_2 transgenes described in (a).$$$



(caption on next page)

Fig. 3. Evaluating drug efficacy against G₄C₂ toxicity: Impacts on lifespan, mobility, and eye degeneration in *Drosophila* models. (a) Lifespan assay on *Drosophila* expressing the G₄C₂ transgene *LDS-(G₄C₂)₄₄* (Genotype: *Elav-Gal4/+;UAS-LDS-(G₄C₂)₄₄.GR-GFP/+*) treated either with Control (black) or TMPyP4 at 100 μ M (green). Survival data were plotted using the Kaplan-Meier method. (b) Lifespan assay on *Drosophila* expressing the G₄C₂ transgene described in (b) treated either with Control (black line) or PJ34 at 5 μ M (red). Survival data were plotted using the Kaplan-Meier method. (c) Quantification of climbing ability in *Drosophila* models at day 10 APE treated either with Control or TMPyP4 at 100 μ M. (Genotype: Control, *Elav-Gal4/+;UAS-luciferase/+* | (*G₄C₂*)₃₀ (II), *Elav-Gal4/UAS-(G₄C₂)₃₀;+/+* | *LDS-(G₄C₂)₄₄, Elav-Gal4/+;UAS-LDS-(G₄C₂)₄₄.GR-GFP/+*). (d) Quantification of climbing ability in *Drosophila* expressing denoted G₄C₂ transgenes described in (c) at day 10 APE treated either with Control or PJ34 at 5 μ M. (e) Representative images of *Drosophila* eye expressing denoted G₄C₂ transgenes at day 10 APE (Genotype: Control, *GMR-Gal4/+;UAS-luciferase/+* | (*G₄C₂*)₃₀ (II), *GMR-Gal4/UAS-(G₄C₂)₃₀;+/+* | *LDS-(G₄C₂)₄₄, GMR-Gal4/+;UAS-LDS-(G₄C₂)₄₄.GR-GFP/+*). The flies were fed with Control (ACDW) or treated with TMPyP4 at 100 μ M (black scale bar, 100 μ m). (f) Quantification of eye degeneration scores in *Drosophila* expressing denoted G₄C₂ transgenes, as described in (e) fed with Control (ACDW) or treated with TMPyP4 at 100 μ M. Eye degeneration was scored based on the criteria provided in [Supplementary Figure S1b](#). (g) Representative images of *Drosophila* eye expressing denoted G₄C₂ transgenes described in [Figure 3e](#) at day 10 APE. The flies were fed with Control (dimethyl sulfoxide, DMSO 0.01%) or treated with PJ34 at 5 μ M. (h) Quantification of the eye phenotype in *Drosophila* expressing denoted G₄C₂ transgenes described in (e), fed with Control (DMSO 0.01%) or treated with PJ34 at 5 μ M. Eye degeneration was scored based on the criteria provided in [Supplementary Figure S1c](#).

localize in distinct subcellular localizations, as previously indicated by [Wen et al. \(2014\)](#).

In our investigation into the pathological markers associated with G₄C₂ repeats expansion, we turned our attention to the mislocalization of TAR DNA-binding protein-43 (TDP-43, also known as TBPH in *Drosophila*), a phenomenon well-documented in various neurodegenerative disorders as well as C9orf72 repeat-associated expansion ([Haeusler et al., 2016](#); [Solomon et al., 2018](#)). Utilizing a previously used TBPH-specific antibody ([Lin et al., 2011](#); [Park et al., 2020](#)), we analyzed the localization patterns of this protein across our fly models within the Kenyon cells. Our observations revealed a shift in TBPH localization under the influence of G₄C₂ expression ([Supplementary Fig. S2b](#)). Contrary to the predominant nuclear presence of TBPH in control cells, models expressing G₄C₂ exhibited a discernible decrease in nucleus TBPH with an increase in cytoplasmic TBPH inclusion, indicating a potential involvement of alterations in the nuclear-cytoplasmic transport mechanisms, a finding that aligns with current scientific discourse on neurodegenerative pathologies ([Gasset-Rosa et al., 2019](#); [Solomon et al., 2018](#)).

Due to previous reports indicating that repeat-associated RNA toxicity may be involved in cellular or behavioral defects ([Cunningham et al., 2020](#); [Goodman et al., 2019b](#); [Kim et al., 2021](#); [McEachin et al., 2020](#)), we quantified the transgene-specific RNA levels in various transgene expressions through quantitative real-time PCR (qRT-PCR) analysis ([Supplementary Fig. S5a-d](#)). Our findings demonstrated a marked increase in RNA transgenes across all measured fly lines, with specific RNA measures correlating with our earlier toxicity profiles ([Fig. 1a-e](#)). This correlation, however, should be approached with a degree of caution due to the methodological challenges in comparing RNA levels across different transgenes (see [Discussion](#)).

Collectively, these results not only support the notion that DPRs, such as GP and GR DPRs, exhibit distinct subcellular localizations and potentially possess varying mechanisms of action but also highlight the consistency of our data with findings from other literature underscoring the reliability of our platform to model G₄C₂-related diseases. Future research is essential to delve deeper into these mechanisms and investigate possible therapeutic strategies to counter G₄C₂-related neurotoxicity.

Evaluating Drug Efficacy Against G₄C₂ Toxicity: Impacts on Lifespan, Mobility, and Eye Degeneration in *Drosophila* Models

In the present investigation, our attention was concentrated primarily on the *LDS-(G₄C₂)₄₄* and (*G₄C₂*)₃₀ (II) transgene constructs. This choice was guided by several factors. Primarily, these models displayed high toxicity levels in the 3 preceding tests (eye degeneration analysis, climbing ability analysis, and lifespan analysis) without reaching lethality, a critical attribute for deriving measurable results. Constructs such as (*G₄C₂*)₄₉ were eliminated from consideration due to their extreme toxicity levels, which led to lethality and thereby precluded further analysis. Conversely, constructs that exhibited weak to moderate toxicity lacked the sensitivity and robustness required for a valuable model to evaluate the potential therapeutic interventions. Similarly, we selected constructs that demonstrated DPR expression, intrigued to investigate potential alterations in DPR expression or localization induced by our therapeutic agents.

We next sought to investigate the potential of specific therapeutic candidates in mitigating these effects ([Supplementary Fig. S3a](#)). As such, we chose 3 compounds, TMPyP4, PJ34, and KPT-276, for evaluation due to their distinct mechanisms of action in relation to different stages of G₄C₂ toxicity. TMPyP4 is known to bind to and destabilize G-quadruplexes, potentially affecting the stability of G₄C₂ repeats and thereby reducing both RNA and protein toxicity ([Zamiri et al., 2014](#)). PJ34 is an inhibitor of poly (adenosine diphosphate-ribose) polymerase and is specifically considered for attenuating protein toxicity ([Gao et al., 2022](#)). KPT-276 inhibits the nuclear export of proteins and RNA and thus might affect G₄C₂-related pathologies through modulating nucleocytoplasmic trafficking ([Chou et al., 2018](#); [Schmidt et al., 2013](#)). This selection of drugs allowed us to target and dissect various aspects of G₄C₂ toxicity.

We first assessed the impact of TMPyP4, PJ34, and KPT-276 on the lifespan of flies expressing the *LDS-(G₄C₂)₄₄* line using *Elav-Gal4* ([Fig. 3a, b](#), [Supplementary Fig. S3b](#)). The dosages administered were based on established concentrations from prior studies using the *Drosophila* ALS models, ensuring methodological consistency and comparability of our results with existing literature ([Chou et al., 2018](#); [Gao et al., 2022](#); [Schmidt et al., 2013](#); [Zamiri et al., 2014](#)). Both TMPyP4 and

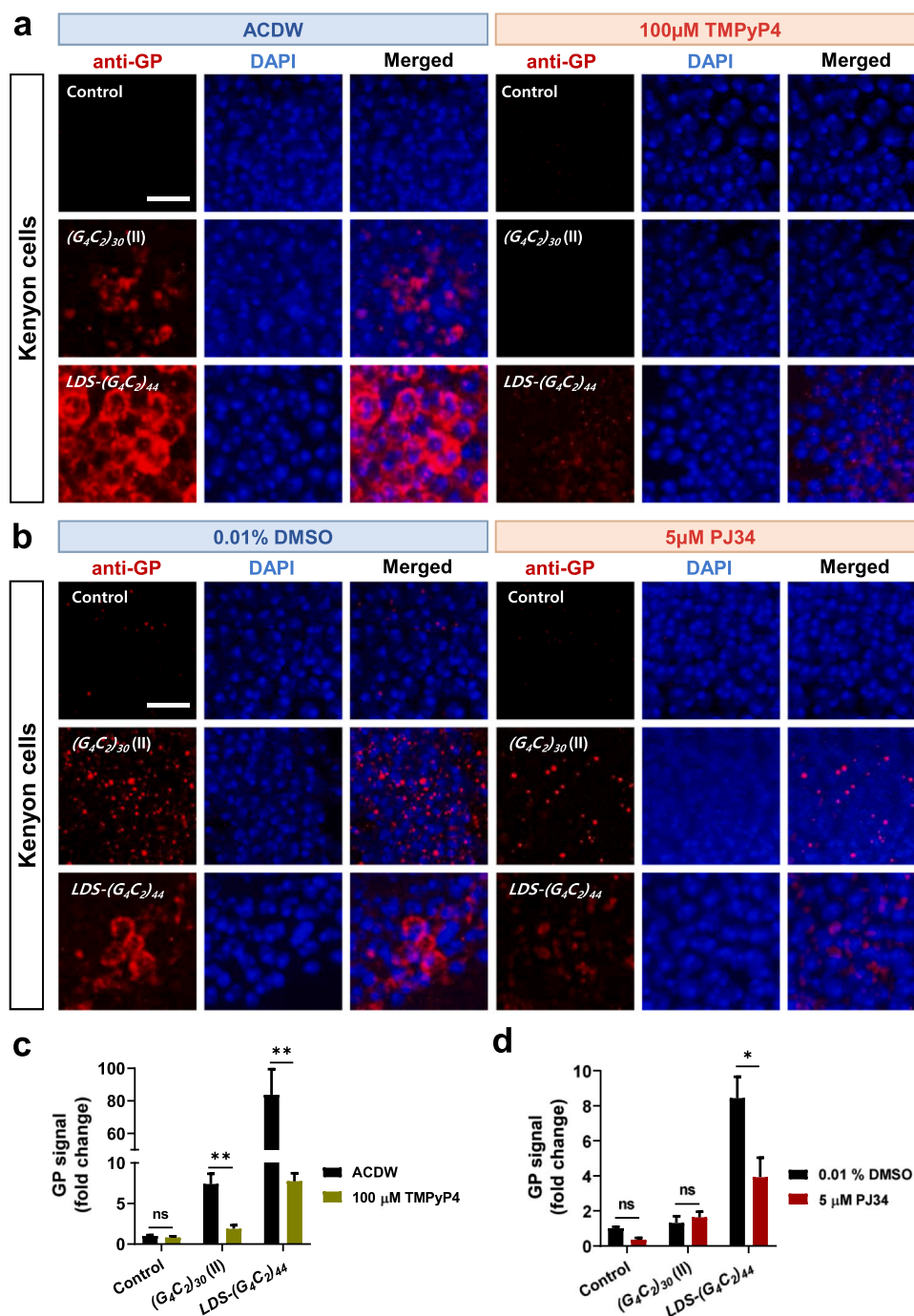


Fig. 4. Impact of representative G_4C_2 -associated drugs on GP DPR in *Drosophila* models. (a) Representative images of GP staining in the Kenyon cells of *Drosophila* brains expressing G_4C_2 transgenes at day 10 APE. (Genotype: Control, *Elav-Gal4/UAS-luciferase/+* | $(G_4C_2)_{30}(II)$, *Elav-Gal4/UAS-(G₄C₂)₃₀+/+* | $LDS-(G_4C_2)_{44}$, *Elav-Gal4/+;UAS-LDS-(G₄C₂)₄₄-GR-GFP/+*). The experimental lines were treated with either ACDW or TMPyP4 at 100 μ M (white scale bar, 5 μ m). (b) Representative images of GP staining in the Kenyon cells of *Drosophila* brains expressing G_4C_2 transgenes denoted in (a) at day 10 APE. The experimental lines were treated with either DMSO (0.01%) or PJ34 at 5 μ M (white scale bar, 5 μ m). (c) Quantification of GP DPR staining in *Drosophila* expressing denoted G_4C_2 transgenes described in (a) treated with either ACDW or TMPyP4 at 100 μ M. (d) Quantification of GP DPR staining in *Drosophila* expressing denoted G_4C_2 transgenes described in (a) treated with either DMSO (0.01%) or PJ34 at 5 μ M.

PJ34 treatments significantly extended the lifespan of these flies compared to controls. However, KPT-276 did not exhibit a notable effect on lifespan (Supplementary Fig. S3b).

Next, we investigated the effects of 3 abovementioned drugs on the climbing ability of flies expressing the $(G_4C_2)_{30}(II)$ and $LDS-(G_4C_2)_{44}$ lines (Fig. 3c, d, Supplementary Fig. S3c). We observed

Reference drugs		TMPyP4		PJ34		KPT-276	
G ₄ C ₂ repeats models		(G ₄ C ₂) ₃₀ (II)	LDS-(G ₄ C ₂) ₄₄	(G ₄ C ₂) ₃₀ (II)	LDS-(G ₄ C ₂) ₄₄	(G ₄ C ₂) ₃₀ (II)	LDS-(G ₄ C ₂) ₄₄
Pathological Outcomes	Eye Degeneration	O	O	O	O	O	X
	Lifespan	N/A	O	N/A	O	N/A	X
	Climbing assay (d3)	O	O	O	X	X	X
	Climbing assay (d10)	O	O	O	X	X	X
Quantity of GP signal		Decrease	Decrease	X	Decrease	X	X
Quantity of GR-GFP signal		N/A	X	N/A	X	N/A	X

Fig. 5. Summary table of the disparate phenotypic outcomes in *Drosophila* expressing (G₄C₂)₃₀ (II) and LDS-(G₄C₂)₄₄ treated with disease-modifying drugs (a) The table presents the differing responses of *Drosophila* expressing (G₄C₂)₃₀ (II) and LDS-(G₄C₂)₄₄ when treated with three previously characterized disease-modifying drugs. The symbols “O” and “X” are utilized to denote an ameliorating effect and no observable change respectively.

that TMPyP4 and PJ34 had beneficial effects on the climbing ability, but only in the (G₄C₂)₃₀ (II) expressing flies. No significant improvement in the climbing ability of the LDS-(G₄C₂)₄₄ line was seen. KPT-276 did not affect the climbing ability of flies expressing the 2 G₄C₂ transgenes (Supplementary Fig. S3c).

Lastly, we used *GMR-Gal4* to express (G₄C₂)₃₀ (II) and LDS-(G₄C₂)₄₄ in the eyes of flies and evaluated the effects of TMPyP4, PJ34, and KPT-276 on eye degeneration (Fig. 3e-h, Supplementary Fig. S3d, S3e) using the degeneration severity criteria detailed in Supplementary Figure S1b and c. Remarkably, all 3 drugs showed a beneficial effect in reducing the degeneration scores for both G₄C₂ constructs, indicating their potential to alleviate eye pathologies associated with G₄C₂ toxicity (with the exception of KPT-276, which alleviated the eye degeneration in (G₄C₂)₃₀ (II) but not LDS-(G₄C₂)₄₄).

Our results indicate that TMPyP4 ameliorates disease phenotype, reinforcing the notion that destabilizing RNA G₄C₂ G-quadruplex structures can inhibit associated toxicity (Li et al., 2021; Mishra et al., 2019). Recent studies have unveiled that an RNA helicase, DHX36, can modulate the toxicity of G₄C₂ by acting on repeat RNA G-quadruplexes and facilitating RAN translation (Liu et al., 2021; Tseng et al., 2021). Given these findings, we were interested in exploring whether genetic modulation of G-quadruplex regulators can affect disease phenotype in our experimental platform. To address this, we generated transgene RNA helicase associated with AU-rich element (Rhau), the *Drosophila* homolog of DHX36, and a potent G-quadruplex unwinder, and coexpressed it with (G₄C₂)₃₀ (II) and observed the *Drosophila* eye degeneration intensity. Our results confirm that the coexpression of Rhau with (G₄C₂)₃₀ (II) did in fact amplify the toxicity, suggesting a role for Rhau in exacerbating the disease phenotype (Supplementary Fig. S3f and g), a finding consistent with previous literature (Liu et al., 2021; Tseng et al., 2021). These results imply that our platform may be applied not only for the testing of pharmacological drugs but also for exploring genetic modulations.

Our data indicate that TMPyP4 and PJ34 can ameliorate some of the toxic effects associated with G₄C₂ constructs, particularly in extending lifespan and improving climbing ability in specific constructs. Moreover, TMPyP4, PJ34, and KPT-276 were all effective in reducing eye degeneration associated with G₄C₂ toxicity. These findings provide valuable insights into potential therapeutic strategies for conditions associated with G₄C₂ repeat expansions and underscore the importance of targeting different aspects of G₄C₂ toxicity.

Impact of Representative G4C2-Associated Drugs on GP DPR in *Drosophila* Models

Given that the 3 previously characterized disease-modifying drugs—TMPyP4, PJ34, and KPT-276—were able to elicit amelioration of G₄C₂-associated toxicity in (G₄C₂)₃₀ (II) and LDS-(G₄C₂)₄₄ expressing flies, we decided to investigate the expression and localization of DPR proteins. We hypothesized that the beneficial effects observed in Figure 3 could potentially result from a change in the localization of -, or the reduction of DPR proteins.

In accordance with this hypothesis, we found that treatment with TMPyP4 at 100 μM led to a reduction in DPR expression in both (G₄C₂)₃₀ (II) and LDS-(G₄C₂)₄₄ lines (Fig. 4a and c). TMPyP4 is a known G-quadruplex destabilizer, and its ability to reduce the expression of DPR proteins suggests that it may be acting through destabilization of the G-quadruplex structures in the G₄C₂ region, thereby inhibiting the aberrant translation process that generates the toxic DPRs (Wang et al., 2019). Similarly, treatment with PJ34 also led to a decrease in GP signals but only in LDS-(G₄C₂)₄₄ lines (Fig. 4b and d). However, PJ34’s effects were not as potent as TMPyP4’s and both were no observable changes in the localization of GP proteins. Interestingly, KPT-276, a selective nuclear export inhibitor, fed flies showed no difference in GP signals in comparison to the control group (Supplementary Fig. S4a and b). It is important to note that all 3 drugs were unable to significantly reduce (or alter

the localization of-; data not shown) GR DPRs, as measured by GFP signals in *LDS-(G₄C₂)₄₄* lines (Supplementary Fig. S4c-f).

Taken together, these data provide evidence that TMPyP4, PJ34, can reduce or ameliorate the toxic effects of G₄C₂ transgenes. Because our study primarily concentrates on the reduction of GP, a commonly recognized non-toxic DPR, it is crucial to extend the research to include the distribution of other DPR proteins, such as GA, PR, or even chimeric DPRs. In addition, it remains inconclusive whether these drugs can reduce GR DPRs in other flies expressing transgenes other than *LDS-(G₄C₂)₄₄*. This exploration would provide a firmer understanding of the effects of the 3-representative disease-modifying drugs.

DISCUSSION

In this study, we utilized available *Drosophila* transgenic models of C9orf72-G₄C₂ mutations for a comprehensive and unbiased examination of the neurotoxic and pathological consequences. Our systematic comparative analysis indicates that these constructs are associated with distinct toxicity profiles, which encompass degenerative effects on the eye, impairment of climbing ability, and a reduction in lifespan, thereby suggesting a well-substantiated model for the exploration of neurodegeneration. Moreover, we present an experimental framework that aids in comprehending how factors, such as subtle sequential differences, may engender significant disparities in both toxicity profiles and drug treatment outcomes (Fig. 5). Although it remains elusive which specific constructs are responsible for higher G₄C₂ expression levels, their differential expression patterns warrant investigation to elucidate the reasons behind variable toxicities among constructs. This knowledge may be pivotal in shaping future research directions.

In addition to DPR toxicity, RNA toxicity may play a role in neurodegeneration. To test this hypothesis, we performed qRT-PCR using construct-specific primers to quantify G₄C₂ RNA levels (Supplementary Fig. S5a-d) within the same category of G₄C₂ transgenes. We found that all tested transgenes showed a significant increase in probed RNA. Interestingly, we found that the (G₄C₂)₃₀ (II) line exhibited higher RNA levels compared to (G₄C₂)₃₀ (III) line, consistent with our toxicity profile data (Supplementary Fig. S5c). However, interpreting these RNA results necessitates caution, primarily since direct quantitative comparison of RNA across different transgenes is methodologically constrained due to inherent variations in used primers for qRT-PCR. These findings suggest the need for further comprehensive studies to delineate the potential toxicity caused by RNA in the context of G₄C₂ expansions and neurodegeneration. Nonetheless, the successful conduction of qRT-PCR using different primers offers promising prospects for advancing our understanding of this complex area of research.

Since all fly brains expressing G₄C₂ repeat-associated transgenes showed increased expression levels of G₄C₂ RNA compared to the control, we were curious to see whether aberrant G₄C₂ expression might precipitate global RNA irregularities. To examine this, we employed rRNA antibodies, which revealed a significant augmentation in cytoplasmic rRNA foci in both (G₄C₂)₃₀ (II) and *LDS-(G₄C₂)₄₄* lines (Supplementary Fig.

S5e and f). This phenotype is particularly interesting in light of prior studies that have underscored that G₄C₂ expression contributes not just to TDP-43 aggregation but also to the formation of RNA foci in the cytoplasm. Nevertheless, we must tread carefully in interpreting the rRNA foci data, as the precise genesis of these structures remains undetermined, and their functional implications within cellular pathology are still to be unraveled. Future studies employing molecular investigations to elucidate the origins and consequential ramifications of rRNA foci formation in relation to G₄C₂ expression will be beneficial in understanding G₄C₂ repeat expansion-associated RNA toxicity.

Beyond the insights gained regarding G₄C₂ toxicity, our *Drosophila* platform demonstrates a promising utility in therapeutic development. As well as providing an effective model for screening potential pharmacological interventions such as TMPyP4, PJ34, and KPT-276, this platform may also serve as a powerful tool for genetic interactor screenings, as exemplified by our findings from *Rhau* expression studies. Genetic screenings can offer critical insights into the molecular mechanisms underlying G₄C₂ toxicity and the pathology of associated diseases. They can identify genetic modifiers, potential risk factors, and potential therapeutic targets, by helping pinpoint genes or genetic interactions that modulate the toxicity of G₄C₂ repeats. Hence, our platform could serve as a resource in the wider scientific community, not only for testing therapeutic efficacy but also for uncovering novel molecular pathways involved in G₄C₂-related pathologies.

The results from our study also shed light on the controversial efficacy of KPT-276. Recent studies have questioned the effectiveness of KPT-276 in improving quality of life in various diseases (Boeynaems et al., 2016; Lee et al., 2016). Our study corroborates these findings, as KPT-276 was found to be ineffective in extending the lifespan or improving the climbing ability of flies expressing *LDS-(G₄C₂)₄₄*. However, we observed a beneficial effect of KPT-276 in reducing eye degeneration in flies expressing the (G₄C₂)₃₀ construct as depicted in a previous study (Zhang et al., 2015). This suggests that while KPT-276 may have a role in certain facets of G₄C₂ toxicity, its therapeutic potential may be limited or context-dependent (Vanneste and Van Den Bosch, 2021). These results lend additional credibility to our platform, demonstrating its capacity to reflect real-world clinical data, and thus reinforcing its reliability as a tool for drug efficacy evaluation.

Our study accentuates the necessity for strategic selection of G₄C₂ constructs in ALS research. Researchers would benefit from consideration of the particular aspect of toxicity or pathological features they seek to investigate. For instance, a construct producing abundant DPRs would be more suitable for studies focusing on protein aggregation, whereas those forming G-quadruplexes might be apt for RNA toxicity studies. By strategically selecting G₄C₂ constructs, researchers can design experiments that more accurately model the specific disease mechanisms and evaluate the efficacy of targeted therapeutic interventions.

In addressing the variations observed in GP amounts between different G₄C₂ models, it is important to note the crucial technical limitations of our study. Our primary evidence for comparing GP expression levels is the GP signal differences

measured through IHC-based imaging techniques, which can be misleading in quantifying protein levels (Fig. 2a and b). Therefore, we performed a western blot analysis using both GP- and GR-specific antibodies in fly brains expressing G₄C₂ repeat constructs to (1) validate the GP- and GR-specific antibodies used for IHC and (2) compare DPR protein quantities between different G₄C₂ models. While we were able to detect GP or GR in *LDS-(G₄C₂)₄₄* expressing flies that harbor a GFP tag in the GR repeat frame (or a single off-framed GFP in the GP repeat frame), thereby suggesting that the GP- and GR-specific antibodies are likely specific and effective, we were unable to detect the measurable amount of GP or GR DPRs in other lines (data not shown). We speculate that the detection of DPRs in *LDS-(G₄C₂)₄₄* expressing flies may stem from the nature of fused GFP, which resulted in increased size and stabilization of *LDS-(G₄C₂)₄₄*-derived GP or GR protein which made it possible to overcome detection threshold of western blot analysis. Additionally, we speculate that the inability to detect GP or GR DPRs in other transgenes expressing flies may be due to the constitution of the G₄C₂ repeat constructs employed in our models. Aside from (G₄C₂)₁₆₀, the constructs used for western blotting analysis were of lengths no greater than 44 repeats, which are likely insufficient for the production of detectable levels of GP or GR proteins. Boivin et al. (2020), encountered similar challenges, reporting an inability to detect DPRs derived from very short G₄C₂ repeats, often less than 10 repeats, even when these sequences were tagged. They hypothesized that such minute DPR proteins likely possess inherent instability, resulting in rapid turnover, which significantly hinders their detectability in standard assay conditions. It is also possible that conventionally used gels or membranes for Western blotting are insufficient in separating and retaining small proteins. This variability necessitates a cautious interpretation of our results. Future studies aiming to quantify DPR levels will benefit from developing enhanced methodologies that can reliably detect and measure smaller or less stable DPR proteins, thereby providing a more comprehensive understanding of their role in ALS/FTD pathology.

It also remains unclear whether these differences in GP signal changes are due to variations in RAN translation efficiency or discrepancies in the transcription levels of the transgenes. It is important to acknowledge that the process of RNA translation is subject to a multitude of influencing factors, including, but not limited to, the availability of ribosomes, the engagement of various initiation factors, specific configurations of mRNA secondary structures, interactions with diverse RNA-binding proteins, and a range of post-transcriptional modifications. Each of these elements can significantly impact the translation process, adding layers of complexity to our understanding of the observed phenomena. Such intricacies in the mechanisms governing RNA translation necessitate a more detailed investigative approach, incorporating advanced kinetics and comprehensive biochemical assays, to unravel the underlying causes of the observed differences in protein levels. Future studies should be conducted to delve deeper into these aspects, potentially utilizing advanced methodologies capable of dissecting the nuanced interplay of factors impacting RNA translation in the context of G₄C₂ repeat expansion.

Our investigation provides a framework for future studies into G₄C₂-associated ALS. Future directions should include evaluating the interplay between G-quadruplexes and DPRs in neuronal toxicity, and how these features can be modulated for therapeutic gains. There is a need for more comprehensive toxicity profiling of the candidate compounds in mammalian models of ALS, including pharmacokinetic and pharmacodynamic assessments. Additionally, the development of high-throughput screening assays utilizing the standardized *Drosophila* constructs could facilitate the identification of novel therapeutic candidates. In conclusion, while the *Drosophila* model offers promising insights and a platform for G₄C₂-associated ALS research, it is essential to acknowledge the complexities and heterogeneity of human pathology. The translation of these findings to human therapeutics, although potentially transformative, necessitates careful and robust validation through in-depth molecular studies and comprehensive clinical trials.

AUTHOR CONTRIBUTIONS

D.L., H.C.J., E.S.K., and S.B.L. wrote the manuscript. H.C.J. and E.S.K. performed experiments. D.L., H.C.J., and E.S.K. analyzed the data. S.Y.K., J.Y.C., S.H.C., K.A.K., J.H.C., B.S.K., I.J.C., C.G.C., E.S.K., and S.B.L. provided expertise and feedback. E.S.K. and S.B.L. supervised the research.

DECLARATION OF COMPETING INTERESTS

The authors have no potential conflicts of interest to disclose.

ACKNOWLEDGMENTS

This work was supported by Basic Science Research Program through the National Research Foundation of Korea (2022R1A4A2000703 and 2021R1A2C1003817) and the Korea Brain Research Institute Research Program (23-BR-03-02), funded by the Ministry of Science and ICT, Republic of Korea and the Korea Health Technology R&D Project through the Korea Health Industry Development Institute and Korea Dementia Research Center (KDRC), funded by the Ministry of Health & Welfare and Ministry of Science and ICT, Republic of Korea (HU21C0027).

APPENDIX A. SUPPLEMENTAL MATERIAL

Supplemental material associated with this article can be found online at: [doi:10.1016/j.mocell.2023.12.003](https://doi.org/10.1016/j.mocell.2023.12.003).

ORCID

Davin Lee <https://orcid.org/0000-0002-1506-5304>
Hae Chan Jeong <https://orcid.org/0009-0008-1184-2445>
Seung Yeol Kim <https://orcid.org/0000-0002-9880-2495>
Jin Yong Chung <https://orcid.org/0009-0009-6025-2895>
Seok Hwan Cho <https://orcid.org/0009-0008-7857-9346>
Kyoung Ah Kim <https://orcid.org/0009-0006-0513-9433>
Jae Ho Cho <https://orcid.org/0000-0002-4037-087X>
Byung Su Ko <https://orcid.org/0009-0009-1667-0985>
In Jun Cha <https://orcid.org/0000-0001-7950-3804>
Chang Geon Chung <https://orcid.org/0000-0001-8155-4926>
Eun Seon Kim <https://orcid.org/0000-0003-4648-5296>
Sung Bae Lee <https://orcid.org/0000-0002-8980-6769>

Received July 28, 2023

Revised November 11, 2023

Accepted November 13, 2023

Available online 15 December 2023.

REFERENCES

- Ash, P.E., Bieniek, K.F., Gendron, T.F., Caulfield, T., Lin, W.L., DeJesus-Hernandez, M., van Blitterswijk, M.M., Jansen-West, K., Paul, J.W., 3rd, Rademakers, R., et al. (2013). Unconventional translation of C9ORF72 GGGGCC expansion generates insoluble polypeptides specific to c9FTD/ALS. *Neuron*, 77, 639-646. <https://doi.org/10.1016/j.neuron.2013.02.004>
- Batra, R., and Lee, C.W. (2017). Mouse models of C9orf72 hexanucleotide repeat expansion in amyotrophic lateral sclerosis/ frontotemporal dementia. *Front. Cell. Neurosci.* 11, 196. <https://doi.org/10.3389/fncel.2017.00196>
- Boeynaems, S., Bogaert, E., Michiels, E., Gijssels, I., Sieben, A., Jovicic, A., De Baets, G., Scheveneels, W., Steyaert, J., Cuijt, I., et al. (2016). Drosophila screen connects nuclear transport genes to DPR pathology in c9ALS/FTD. *Sci. Rep.* 6, 20877. <https://doi.org/10.1038/srep20877>
- Boivin, M., Pfister, V., Gaucherot, A., Ruffenach, F., Negroni, L., Sellier, C., and Charlet-Berguerand, N. (2020). Reduced autophagy upon C9ORF72 loss synergizes with dipeptide repeat protein toxicity in G4C2 repeat expansion disorders. *EMBO J.* 39, Article e100574. <https://doi.org/10.15252/embj.2018100574>
- Byrne, S., Heverin, M., Elamin, M., Bede, P., Lynch, C., Kenna, K., MacLaughlin, R., Walsh, C., Al Chalabi, A., and Hardiman, O. (2013). Aggregation of neurologic and neuropsychiatric disease in amyotrophic lateral sclerosis kindreds: a population-based case-control cohort study of familial and sporadic amyotrophic lateral sclerosis. *Ann. Neurol.* 74, 699-708. <https://doi.org/10.1002/ana.23969>
- Cho, J.H., Jo, M.G., Kim, E.S., Lee, N.Y., Kim, S.H., Chung, C.G., Park, J.H., and Lee, S.B. (2022). CBP-mediated acetylation of importin alpha mediates calcium-dependent nucleocytoplasmic transport of selective proteins in Drosophila neurons. *Mol. Cells*, 45, 855-867. <https://doi.org/10.14348/molcells.2022.0104>
- Chou, C.C., Zhang, Y., Umoh, M.E., Vaughan, S.W., Lorenzini, I., Liu, F., Sayegh, M., Donlin-Asp, P.G., Chen, Y.H., Duong, D.M., et al. (2018). TDP-43 pathology disrupts nuclear pore complexes and nucleocytoplasmic transport in ALS/FTD. *Nat. Neurosci.* 21, 228-239. <https://doi.org/10.1038/s41593-017-0047-3>
- Chung, C.G., Kwon, M.J., Jeon, K.H., Hyeon, D.Y., Han, M.H., Park, J.H., Cha, I.J., Cho, J.H., Kim, K., Rho, S., et al. (2017). Golgi outpost synthesis impaired by toxic polyglutamine proteins contributes to dendritic pathology in neurons. *Cell Rep.* 20, 356-369. <https://doi.org/10.1016/j.celrep.2017.06.059>
- Cunningham, K.M., Maulding, K., Ruan, K., Senturk, M., Grima, J.C., Sung, H., Zuo, Z., Song, H., Gao, J., Dubey, S., et al. (2020). TFEB/Mitf links impaired nuclear import to autophagolysosomal dysfunction in C9-ALS. *Elife*, 9. <https://doi.org/10.7554/eLife.59419>
- Dafinca, R., Scaber, J., Ababneh, N., Lalic, T., Weir, G., Christian, H., Vowles, J., Douglas, A.G., Fletcher-Jones, A., Browne, C., et al. (2016). C9orf72 hexanucleotide expansions are associated with altered endoplasmic reticulum calcium homeostasis and stress granule formation in induced pluripotent stem cell-derived neurons from patients with amyotrophic lateral sclerosis and frontotemporal dementia. *Stem Cells*, 34, 2063-2078. <https://doi.org/10.1002/stem.2388>
- DeJesus-Hernandez, M., Mackenzie, I.R., Boeve, B.F., Boxer, A.L., Baker, M., Rutherford, N.J., Nicholson, A.M., Finch, N.A., Flynn, H., Adamson, J., et al. (2011). Expanded GGGGCC hexanucleotide repeat in noncoding region of C9ORF72 causes chromosome 9p-linked FTD and ALS. *Neuron*, 72, 245-256. <https://doi.org/10.1016/j.neuron.2011.09.011>
- Devenney, E., Hornberger, M., Irish, M., Mioshi, E., Burrell, J., Tan, R., Kiernan, M.C., and Hodges, J.R. (2014). Frontotemporal dementia associated with the C9ORF72 mutation: a unique clinical profile. *JAMA Neurol.* 71, 331-339. <https://doi.org/10.1001/jamaneurol.2013.6002>
- Dubey, S.K., Maulding, K., Sung, H., and Lloyd, T.E. (2022). Nucleoporins are degraded via upregulation of ESCRT-III/Vps4 complex in Drosophila models of C9-ALS/FTD. *Cell Rep.* 40, Article 111379. <https://doi.org/10.1016/j.celrep.2022.111379>
- Gao, J., Mewborne, Q.T., Girdhar, A., Sheth, U., Coyne, A.N., Punathil, R., Kang, B.G., Dasovich, M., Veire, A., DeJesus Hernandez, M., et al. (2022). Poly(ADP-ribose) promotes toxicity of C9ORF72 arginine-rich dipeptide repeat proteins. *Sci. Transl. Med.* 14, Article eabq3215. <https://doi.org/10.1126/scitranslmed.abq3215>
- Gasset-Rosa, F., Lu, S., Yu, H., Chen, C., Melamed, Z., Guo, L., Shorter, J., Da Cruz, S., and Cleveland, D.W. (2019). Cytoplasmic TDP-43 de-mixing independent of stress granules drives inhibition of nuclear import, loss of nuclear TDP-43, and cell death. *Neuron*, 102, 339-357. <https://doi.org/10.1016/j.neuron.2019.02.038>
- Goodman, L.D., Prudencio, M., Kramer, N.J., Martinez-Ramirez, L.F., Srinivasan, A.R., Lan, M., Parisi, M.J., Zhu, Y., Chew, J., Cook, C.N., et al. (2019). Toxic expanded GGGGCC repeat transcription is mediated by the PAF1 complex in C9orf72-associated FTD. *Nat. Neurosci.* 22, 863-874. <https://doi.org/10.1038/s41593-019-0396-1>
- Goodman, L.D., Prudencio, M., Srinivasan, A.R., Rifai, O.M., Lee, V.M., Petrucelli, L., and Bonini, N.M. (2019). eIF4B and eIF4H mediate GR production from expanded G4C2 in a Drosophila model for C9orf72-associated ALS. *Acta Neuropathol. Commun.* 7, Article 62. <https://doi.org/10.1186/s40478-019-0711-9>
- Haeusler, A.R., Donnelly, C.J., and Rothstein, J.D. (2016). The expanding biology of the C9orf72 nucleotide repeat expansion in neurodegenerative disease. *Nat. Rev. Neurosci.* 17, 383-395. <https://doi.org/10.1038/nrn.2016.38>
- Kearse, M.G., Green, K.M., Krans, A., Rodriguez, C.M., Linsalata, A.E., Goldstrohm, A.C., and Todd, P.K. (2016). CGG repeat-associated non-AUG translation utilizes a Cap-dependent scanning mechanism of initiation to produce toxic proteins. *Mol. Cell*, 62, 314-322. <https://doi.org/10.1016/j.molcel.2016.02.034>
- Kim, E.S., Chung, C.G., Park, J.H., Ko, B.S., Park, S.S., Kim, Y.H., Cha, I.J., Kim, J., Ha, C.M., Kim, H.J., et al. (2021). C9orf72-associated arginine-rich dipeptide repeats induce RNA-dependent nuclear accumulation of Staufen in neurons. *Hum. Mol. Genet.* 30, 1084-1100. <https://doi.org/10.1093/hmg/ddab089>
- Kramer, N.J., Carlomagno, Y., Zhang, Y.J., Almeida, S., Cook, C.N., Gendron, T.F., Prudencio, M., Van Blitterswijk, M., Belzil, V., Couthouis, J., et al. (2016). Spt4 selectively regulates the expression of C9orf72 sense and antisense mutant transcripts. *Science*, 353, 708-712. <https://doi.org/10.1126/science.aaf7791>
- Kwiatkowski, T.J., Jr., Bosco, D.A., Leclerc, A.L., Tamrazian, E., Vanderburg, C.R., Russ, C., Davis, A., Gilchrist, J., Kasarskis, E.J., Munsat, T., et al. (2009). Mutations in the FUS/TLS gene on chromosome 16 cause familial amyotrophic lateral sclerosis. *Science*, 323, 1205-1208. <https://doi.org/10.1126/science.1166066>
- Lee, J., Song, X., Hyun, B., Jeon, C.O., and Hyun, S. (2023). Drosophila gut immune pathway suppresses host development-promoting effects

- of acetic acid bacteria. *Mol. Cells*, **46**, 637-653. <https://doi.org/10.14348/molcells.2023.0141>
- Lee, K.H., Zhang, P., Kim, H.J., Mitrea, D.M., Sarkar, M., Freibaum, B.D., Cika, J., Coughlin, M., Messing, J., Molliex, A., et al. (2016). C9orf72 dipeptide repeats impair the assembly, dynamics, and function of membrane-less organelles. *Cell*, **167**, 774-788. <https://doi.org/10.1016/j.cell.2016.10.002>
- Lee, Y., Kim, J., Kim, H., Han, J.E., Kim, S., Kang, K.H., Kim, D., Kim, J.M., and Koh, H. (2022). Pyruvate dehydrogenase kinase protects dopaminergic neurons from oxidative stress in drosophila DJ-1 null mutants. *Mol. Cells*, **45**, 454-464. <https://doi.org/10.14348/molcells.2022.5002>
- Lee, Y.B., Chen, H.J., Peres, J.N., Gomez-Deza, J., Attig, J., Stalekar, M., Troakes, C., Nishimura, A.L., Scotter, E.L., Vance, C., et al. (2013). Hexanucleotide repeats in ALS/FTD form length-dependent RNA foci, sequester RNA binding proteins, and are neurotoxic. *Cell Rep.* **5**, 1178-1186. <https://doi.org/10.1016/j.celrep.2013.10.049>
- Li, C., Wu, B., Chen, S., Hao, K., Yang, J., Cao, H., Yang, S., Wu, Z.S., and Shen, Z. (2021). Structural requirement of G-quadruplex/aptamer-combined DNA macromolecule serving as efficient drug carrier for cancer-targeted drug delivery. *Eur. J. Pharm. Biopharm.* **159**, 221-227. <https://doi.org/10.1016/j.ejpb.2020.11.021>
- Lin, M.J., Cheng, C.W., and Shen, C.K. (2011). Neuronal function and dysfunction of Drosophila dTDP. *PLoS One*, **6**, Article e20371. <https://doi.org/10.1371/journal.pone.0020371>
- Liu, H., Lu, Y.N., Paul, T., Periz, G., Banco, M.T., Ferre-D'Amare, A.R., Rothstein, J.D., Hayes, L.R., Myong, S., and Wang, J. (2021). A helicase unwinds hexanucleotide repeat RNA G-quadruplexes and facilitates repeat-associated non-AUG translation. *J. Am. Chem. Soc.* **143**, 7368-7379. <https://doi.org/10.1021/jacs.1c00131>
- Majounie, E., Renton, A.E., Mok, K., Dopper, E.G., Waite, A., Rollinson, S., Chio, A., Restagno, G., Nicolaou, N., Simon-Sanchez, J., et al. (2012). Frequency of the C9orf72 hexanucleotide repeat expansion in patients with amyotrophic lateral sclerosis and frontotemporal dementia: a cross-sectional study. *Lancet Neurol.* **11**, 323-330. [https://doi.org/10.1016/S1474-4422\(12\)70043-1](https://doi.org/10.1016/S1474-4422(12)70043-1)
- McEachin, Z.T., Parameswaran, J., Raj, N., Bassell, G.J., and Jiang, J. (2020). RNA-mediated toxicity in C9orf72 ALS and FTD. *Neurobiol. Dis.* **145**, Article 105055. <https://doi.org/10.1016/j.nbd.2020.105055>
- Mishra, S.K., Shankar, U., Jain, N., Sikri, K., Tyagi, J.S., Sharma, T.K., Mergny, J.L., and Kumar, A. (2019). Characterization of G-quadruplex motifs in espB, espK, and cyp51 genes of *Mycobacterium tuberculosis* as potential drug targets. *Mol. Ther. Nucleic Acids*, **16**, 698-706. <https://doi.org/10.1016/j.omtn.2019.04.022>
- Mizielinska, S., Gronke, S., Niccoli, T., Ridler, C.E., Clayton, E.L., Devoy, A., Moens, T., Norona, F.E., Woollacott, I.O.C., Pietrzyk, J., et al. (2014). C9orf72 repeat expansions cause neurodegeneration in Drosophila through arginine-rich proteins. *Science*, **345**, 1192-1194. <https://doi.org/10.1126/science.1256800>
- Park, J.H., Chung, C.G., Park, S.S., Lee, D., Kim, K.M., Jeong, Y., Kim, E.S., Cho, J.H., Jeon, Y.M., Shen, C.J., et al. (2020). Cytosolic calcium regulates cytoplasmic accumulation of TDP-43 through Calpain-A and Importin alpha3. *Elife*, **9**. <https://doi.org/10.7554/eLife.60132>
- Pradhan, R.N., Shrestha, B., and Lee, Y. (2023). Molecular basis of hexanoic acid taste in *Drosophila melanogaster*. *Mol. Cells*, **46**, 451-460. <https://doi.org/10.14348/molcells.2023.0035>
- Rosen, D.R., Siddique, T., Patterson, D., Figlewicz, D.A., Sapp, P., Hentati, A., Donaldson, D., Goto, J., O'Regan, J.P., Deng, H.X., et al. (1993). Mutations in Cu/Zn superoxide dismutase gene are associated with familial amyotrophic lateral sclerosis. *Nature*, **362**, 59-62. <https://doi.org/10.1038/362059a0>
- Ryu, T.H., Subramanian, M., Yeom, E., and Yu, K. (2022). The prominin-like gene expressed in a subset of dopaminergic neurons regulates locomotion in Drosophila. *Mol. Cells*, **45**, 640-648. <https://doi.org/10.14348/molcells.2022.0006>
- Schmidt, J., Braggio, E., Kortuem, K.M., Egan, J.B., Zhu, Y.X., Xin, C.S., Tiedemann, R.E., Palmer, S.E., Garbitt, V.M., McCauley, D., et al. (2013). Genome-wide studies in multiple myeloma identify XPO1/CRM1 as a critical target validated using the selective nuclear export inhibitor KPT-276. *Leukemia*, **27**, 2357-2365. <https://doi.org/10.1038/leu.2013.172>
- Shatunov, A., Mok, K., Newhouse, S., Weale, M.E., Smith, B., Vance, C., Johnson, L., Veldink, J.H., van Es, M.A., van den Berg, L.H., et al. (2010). Chromosome 9p21 in sporadic amyotrophic lateral sclerosis in the UK and seven other countries: a genome-wide association study. *Lancet Neurol.* **9**, 986-994. [https://doi.org/10.1016/S1474-4422\(10\)70197-6](https://doi.org/10.1016/S1474-4422(10)70197-6)
- Shi, Y., Lin, S., Staats, K.A., Li, Y., Chang, W.H., Hung, S.T., Hendricks, E., Linares, G.R., Wang, Y., Son, E.Y., et al. (2018). Haploinsufficiency leads to neurodegeneration in C9ORF72 ALS/FTD human induced motor neurons. *Nat. Med.* **24**, 313-325. <https://doi.org/10.1038/nm.4490>
- Solomon, D.A., Stepto, A., Au, W.H., Adachi, Y., Diaper, D.C., Hall, R., Rekhi, A., Boudi, A., Tziortzouda, P., Lee, Y.B., et al. (2018). A feedback loop between dipeptide-repeat protein, TDP-43 and karyopherin-alpha mediates C9orf72-related neurodegeneration. *Brain*, **141**, 2908-2924. <https://doi.org/10.1093/brain/awy241>
- Tran, H., Almeida, S., Moore, J., Gendron, T.F., Chalasani, U., Lu, Y., Du, X., Nickerson, J.A., Petrucelli, L., Weng, Z., et al. (2015). Differential toxicity of nuclear RNA foci versus dipeptide repeat proteins in a Drosophila model of C9ORF72 FTD/ALS. *Neuron*, **87**, 1207-1214. <https://doi.org/10.1016/j.neuron.2015.09.015>
- Tseng, Y.J., Sandwith, S.N., Green, K.M., Chambers, A.E., Krans, A., Raimor, H.M., Sharlow, M.E., Reisinger, M.A., Richardson, A.E., Routh, E.D., et al. (2021). The RNA helicase DHX36-G4R1 modulates C9orf72 GGGGCC hexanucleotide repeat-associated translation. *J. Biol. Chem.* **297**, Article 100914. <https://doi.org/10.1016/j.jbc.2021.100914>
- Van Daele, S.H., Moisse, M., van Vugt, J., Zwamborn, R.A.J., van der Spek, R., van Rheenen, W., Van Eijk, K., Kenna, K., Corcia, P., Vourc'h, P., et al. (2023). Genetic variability in sporadic amyotrophic lateral sclerosis. *Brain*, **146**, 3760-3769. <https://doi.org/10.1093/brain/awad120>
- Vanneste, J., and Van Den Bosch, L. (2021). The role of nucleocytoplasmic transport defects in amyotrophic lateral sclerosis. *Int. J. Mol. Sci.* **22**. <https://doi.org/10.3390/ijms222212175>
- Wang, Z.F., Ursu, A., Childs-Disney, J.L., Guertler, R., Yang, W.Y., Bernat, V., Rzuczek, S.G., Fuerst, R., Zhang, Y.J., Gendron, T.F., et al. (2019). The hairpin form of r(G(4)C(2))(exp) in c9ALS/FTD is repeat-associated non-ATG translated and a target for bioactive small molecules. *Cell. Chem. Biol.* **26**, 179-190. <https://doi.org/10.1016/j.chembiol.2018.10.018>
- Wen, X., An, P., Li, H., Zhou, Z., Sun, Y., Wang, J., Ma, L., and Lu, B. (2020). Tau accumulation via reduced autophagy mediates GGGGCC repeat expansion-induced neurodegeneration in Drosophila model of ALS. *Neurosci. Bull.* **36**, 1414-1428. <https://doi.org/10.1007/s12264-020-00518-2>
- Wen, X., Tan, W., Westergard, T., Krishnamurthy, K., Markandaiah, S.S., Shi, Y., Lin, S., Shneider, N.A., Monaghan, J., Pandey, U.B., et al. (2014). Antisense proline-arginine RAN dipeptides linked to C9ORF72-ALS/FTD form toxic nuclear aggregates that initiate in vitro and in vivo neuronal death. *Neuron*, **84**, 1213-1225. <https://doi.org/10.1016/j.neuron.2014.12.010>

- Xu, Z., Poidevin, M., Li, X., Li, Y., Shu, L., Nelson, D.L., Li, H., Hales, C.M., Gearing, M., Wingo, T.S., et al. (2013). Expanded GGGGCC repeat RNA associated with amyotrophic lateral sclerosis and frontotemporal dementia causes neurodegeneration. *Proc. Natl. Acad. Sci. U.S.A.* 110, 7778-7783. <https://doi.org/10.1073/pnas.1219643110>
- Yuva-Aydemir, Y., Almeida, S., Krishnan, G., Gendron, T.F., and Gao, F.B. (2019). Transcription elongation factor AFF2/FMR2 regulates expression of expanded GGGGCC repeat-containing C9ORF72 allele in ALS/FTD. *Nat. Commun.* 10, Article 5466. <https://doi.org/10.1038/s41467-019-13477-8>
- Zamiri, B., Reddy, K., Macgregor, R.B., Jr., and Pearson, C.E. (2014). TMPyP4 porphyrin distorts RNA G-quadruplex structures of the disease-associated r(GGGGCC)_n repeat of the C9orf72 gene and blocks interaction of RNA-binding proteins. *J. Biol. Chem.* 289, 4653-4659. <https://doi.org/10.1074/jbc.C113.502336>
- Zhang, K., Donnelly, C.J., Haeusler, A.R., Grima, J.C., Machamer, J.B., Steinwald, P., Daley, E.L., Miller, S.J., Cunningham, K.M., Vidensky, A., et al. (2015). The C9orf72 repeat expansion disrupts nucleocytoplasmic transport. *Nature*, 525, 56-61. <https://doi.org/10.1038/nature14973>
- Zu, T., Liu, Y., Banez-Coronel, M., Reid, T., Pletnikova, O., Lewis, J., Miller, T.M., Harms, M.B., Falchook, A.E., Subramony, S.H., et al. (2013). RAN proteins and RNA foci from antisense transcripts in C9ORF72 ALS and frontotemporal dementia. *Proc. Natl. Acad. Sci. U.S.A.* 110, E4968-E4977. <https://doi.org/10.1073/pnas.1315438110>